Preconditioned lattice-Boltzmann method for steady flows

Zhaoli Guo, T. S. Zhao,* and Yong Shi
Department of Mechanical Engineering, The Hong Kong University of Science and Technology, Kowloon, Hong Kong
(Received 1 July 2004; published 21 December 2004)

In this paper we propose a preconditioned lattice Boltzmann (LB) method for steady incompressible flows. For steady flows, the macroscopic equations derived from this LB model are equivalent to those from the standard LB model, but with an improved eigenvalue system. The proposed model can be viewed as an explicit solver for preconditioned compressible Navier-Stokes equations. Linear stability analysis is performed and the results show that the stability of the model is the same as that of the standard LB model for low Mach numbers. The proposed model retains the structure of the standard LB model and, hence, possesses all the advantages. Numerical tests show that the convergence rate can be enhanced as much as an order of magnitude compared to the standard lattice Boltzmann method. The accuracy of the solutions is improved as well.

DOI: 10.1103/PhysRevE.70.066706 PACS number(s): 47.11.+j, 02.60.Cb, 02.70.Bf

I. INTRODUCTION

The lattice-Boltzmann method (LBM) developed about a decade ago is a kinetic approach for computational fluid dynamics (CFD) [1–5]. In the LBM, the dynamic behavior of a fluid is described by a lattice-Boltzmann equation (LBE) for the single-particle distribution function (DF), and the flow variables, such as density, velocity, and temperature, are determined from the DF directly. The advantages of the LBM, such as its parallelism, simple structure, simplicity in coding, and the straightforward incorporation of microscopic interactions, have been well demonstrated in the literature. As applied to steady flows, however, the standard LBE usually converges rather slowly [6], and the time-exhausting convergence progress prevents it from being as competitive as conventional CFD methods in practical applications.

The slow convergence rate is an inherent disadvantage of the standard LBM. It is well understood that the LBM is an explicit time-marching method for compressible fluid flows with low Mach numbers, in other words, an explicit artificial compressible scheme for incompressible Navier-Stokes equations. In addition to the error due to numerical discretization, the finite Mach number effect also introduces a grid-independent "compressibility" error. To reduce this error, the Mach number must be sufficiently small in the LBM. As the Mach number becomes smaller, however, it would become increasingly difficult to solve the compressible Navier-Stokes equations using a general time-marching numerical scheme. This difficulty is rooted in the large disparity between the acoustic wave speed and the fluid speed that converts other waves in low Mach number flows [7–10]. Usually, for any explicit scheme, the Courant-Friedrich-Levy (CFL) condition should be fulfilled for the sake of numerical stability. Therefore, the time step should be chosen such that it is inversely proportional to the sound speed of the acoustic wave, during which the waves driven by the fluid change slightly. As a result, a large number of time steps are needed to reach the steady state of the flow. As an explicit scheme, the LBM also suffers from this problem. Researchers have noted this problem and made efforts to accelerate the convergence rate of the LBM from different viewpoints [11–20].

In general, the existing accelerated LBE models fall into two categories: a time-dependent approach and a time-independent approach. In the former, the LBE still evolves as a time-marching process, but the evolution equation is altered either by including a false forcing term into the standard LBE, which accelerates the convergence while it vanishes at the steady state [11,12], or by employing certain implicit schemes to discretize the time-dependent discrete-velocity Boltzmann equation (DVBE) so that a large time step can be used [13–15]. On the other hand, in the time-independent approach, a linear or nonlinear algebra system derived from the time-independent form of the standard LBE or DVBE is solved directly for steady Stokes [16] or Navier-Stokes flows [17–19]. Alternatively, Tölke *et al.* attempted to solve the time-independent DVBE using the multigrid method directly [20].

The accelerated LBMs mentioned above all yield improved convergence in comparison to the standard LBE. These methods, however, are more complicated than the standard LBE, and, thus, the advantage of simplicity of the LBM is sacrificed. In this paper, we aim to propose an LBE model for steady flows that retains the advantages of the standard LBM, but with an accelerated convergence rate. The key point of the model is to modify the equilibrium distribution function (EDF) with the addition of a parameter. With this EDF, the macroscopic equations derived from the model can be viewed as certain preconditioned Navier-Stokes equations [7–10], which are equivalent to the Navier-Stokes equations for steady flows, but with a better solvable condition due to the removal of the original eigenvalue stiffness. The rest of the paper is organized as follows. First, we outline the essential ingredients of the LBM in Sec. II, followed by presenting the LBE model for the steady Navier-Stokes equations in low Mach number limit in Sec. III. Numerical results predicted by this model are compared with the standard time-dependent LBE in Sec. IV. Finally a discussion is made in Sec. V.

*Corresponding author. Email address: metzhao@ust.hk

II. LATTICE-BOLTZMANN EQUATION

The lattice-Boltzmann equation for isothermal flows is a discrete Boltzmann equation with a finite discrete velocity set,

$$f_i(\boldsymbol{x}+\boldsymbol{c}_i\delta_t,t+\delta_t)-f_i(\boldsymbol{x},t)=\Omega_i(f), \tag{1}$$

where $f_i(x,t)$ is the single-particle distribution function for particles moving with velocity $\boldsymbol{c}_i$ at position x and time t, δ_t is time step, and Ω_i is the collision operator representing the rate of change due to collisions in the DF f_i. The most widely used collision operator in LBM is the Bhatnagar-Gross-Krook (BGK) or the single-relaxation-time model,

$$\Omega_i(f)=-\frac{1}{\tau_s}[f_i-f_i^{(eq)}], \tag{2}$$

where τ_s is the nondimensional relaxation time, and $f_i^{(eq)}$ is the local equilibrium distribution function. The macroscopic density ρ and velocity $\boldsymbol{u}$ of the fluid are determined by the particle velocity moments of the DFs,

$$\rho=\sum f_i, \quad \rho\boldsymbol{u}=\sum \boldsymbol{c}_i f_i. \tag{3}$$

The discrete velocities and EDF must be chosen properly such that the mass and momentum are conserved and symmetry requirements are satisfied. As such, the resulting macroscopic equations derived from Eq. (1) describe the correct hydrodynamics of the fluid. For illustration, we now use the D2Q9 model [21] as an example, where the EDF is defined by

$$f_i^{(eq)}=\omega_i\rho\left[1+\frac{\boldsymbol{c}_i\cdot\boldsymbol{u}}{c_s^2}+\frac{\boldsymbol{uu}:(\boldsymbol{c}_i\boldsymbol{c}_i-c_s^2\boldsymbol{I})}{2c_s^4}\right], \tag{4}$$

where the discrete velocities are given by $\boldsymbol{c}_0=\boldsymbol{0}$, and $\boldsymbol{c}_i=\lambda_i(\cos\theta_i,\sin\theta_i)$ with $\lambda_i=c$, $\theta_i=(i-1)\pi/2$ for $i=1-4$, and $\lambda_i=\sqrt{2}c$, $\theta_i=(i-5)\pi/2+\pi/4$ for $i=5-8$. The weights are given by $\omega_0=4/9$, $\omega_i=1/9$ for $i=1-4$, $\omega_i=1/36$ for $i=5-8$, and $c_s=c/\sqrt{3}$ is the sound speed of the model, and $c=\delta_x/\delta_t$, where δ_x is the lattice spacing. The EDF (4) can also be derived from the Boltzmann-Maxwellian distribution via a Taylor expansion in $\boldsymbol{u}/c_s\approx M$ up to second order [22,23], where M represents the Mach number. This indicates that EDF (4) holds only for small M. Therefore, M must be small in the LBM.

The macroscopic equations can be derived from the LBE (1) through the Chapman-Enskog procedure in the low Mach number limit [24]. By neglecting the terms $O(\delta_x M^3)$ and $O(\delta_x^2)$, the derived macroscopic equations can be written as

$$\frac{\partial\rho}{\partial t}+\nabla\cdot(\rho\boldsymbol{u})=0, \tag{5a}$$

$$\frac{\partial(\rho\boldsymbol{u})}{\partial t}+\nabla\cdot(\rho\boldsymbol{uu})=-\nabla p+\nabla\cdot(\rho\nu\boldsymbol{S}), \tag{5b}$$

where $\boldsymbol{S}=\nabla\boldsymbol{u}+(\nabla\boldsymbol{u})^T$, $p=c_s^2\rho$ is the pressure, and the shear viscosity ν is given by

$$\nu=c_s^2\left(\tau_s-\tfrac{1}{2}\right)\delta_t. \tag{6}$$

Since Eqs. (5) take the form of compressible Navier-Stokes equations, the LBE (1) is virtually a solver for isothermal compressible fluid flows with a low Mach number. Compared with the incompressible Navier-Stokes equations, Eqs. (5) have additional terms of order $O(M^2)$ in the continuity equation and $O(M^3)$ in the momentum equation. As we apply the LBM to solve the incompressible Navier-Stokes equations, a "compressible" error, in addition to the usual spacial and temporal discretization errors, arises [25]. Therefore, in practical applications, the Mach number in the LBM should be kept small in order to reduce this error.

Yet, a small Mach number may cause numerical difficulties for the LBM as follows. First, for a flow at a fixed Reynolds number $\mathrm{Re}=LU_0/\nu$, where L and U_0 are the characteristic length and velocity of the flow, from Eq. (6) we obtain

$$\tau_s-0.5=\frac{U_0}{c_s}\frac{L}{\delta_x}\frac{\sqrt{3}}{\mathrm{Re}}=\frac{\sqrt{3}NM}{\mathrm{Re}}, \tag{7}$$

where N is the number of grid points in one direction. Therefore, for a given lattice, τ_s approaches 0.5 as M approaches to zero. It is understood that under this circumstance the computation of the LBE usually becomes unstable [26].

Second, a small Mach number means that LBE usually takes a long time to reach a steady state for a steady flow. This is due to the eigenvalue stiffness of the compressible Navier-Stokes equations (5) [7]. To see this more clearly, we rewrite the two-dimensional Eq. (5) in a vector form,

$$\frac{\partial\boldsymbol{Q}}{\partial t}+\frac{\partial\boldsymbol{E}}{\partial x}+\frac{\partial\boldsymbol{F}}{\partial y}=\boldsymbol{R}\{\boldsymbol{Q}_v\}, \tag{8}$$

where $\boldsymbol{R}$ represents the vector associated with the appropriate viscous terms on the right hand side of Eq. (5), and $\boldsymbol{Q}=(\rho,\rho u,\rho v)^T$, $\boldsymbol{E}=(\rho u,\rho u^2+c_s^2\rho,\rho uv)^T$, $\boldsymbol{F}=(\rho v,\rho uv,\rho v^2+c_s^2\rho)^T$, $\boldsymbol{Q}_v=(0,u,v)^T$, where u and v are the x and y components of the velocity $\boldsymbol{u}$, respectively. Eq. (8) can be further written as

$$\frac{\partial\boldsymbol{Q}}{\partial t}+\boldsymbol{A}\frac{\partial\boldsymbol{Q}}{\partial x}+\boldsymbol{B}\frac{\partial\boldsymbol{Q}}{\partial y}=\boldsymbol{R}\{\boldsymbol{Q}_v\}, \tag{9}$$

where $\boldsymbol{A}=\partial\boldsymbol{E}/\partial\boldsymbol{Q}$ and $\boldsymbol{B}=\partial\boldsymbol{F}/\partial\boldsymbol{Q}$.

It can be shown that the eigenvalues of the matrixes $\boldsymbol{A}$ and $\boldsymbol{B}$ are

$$\lambda(\boldsymbol{A})=(u,u\pm c_s), \quad \lambda(\boldsymbol{B})=(v,v\pm c_s) \tag{10}$$

respectively. Therefore, the condition number of $\boldsymbol{A}$, $\kappa k(\boldsymbol{A})\equiv\max\lambda_i/\lambda_j$ over all the eigenvalues λ of $\boldsymbol{A}$, is of order $1/M$, which will be very large as the Mach number of the flow is small. Similarly, the condition number of matrix $\boldsymbol{B}$ is also large in this case. This fact means that the waves in the fluid transfer with quite different speeds, which will make a time-marching scheme, including the LBE (1), converge very slowly [7]. It is noted that the viscous terms also have complex influences on the wave speeds, depending on the Reynolds number and the ratio of the Reynolds number to the Mach number [9]. The convergence difficulty can be further exacerbated by the magnitude of the diffusion terms [7].

III. PRECONDITIONED LBE

The arguments presented in Sec. II show that the LBE method can be viewed as a time-marching solver for compressible Navier-Stokes equations in the low Mach number limit. From the standpoint of reducing the "compressible" error, the LBM is more applicable to small Mach number flows. A small Mach number, however, may induce numerical difficulties. In particular, for steady flows, a small Mach number causes the convergence to become very slow. To overcome this problem, we propose a preconditioned LBM in this section.

A. Formulation

The preconditioned LBE (PLBE) takes the same form as the standard LBE and is rewritten here as

$$f_i(\boldsymbol{x}+\boldsymbol{c}_i\delta_t,t+\delta_t)-f_i(\boldsymbol{x},t)=-\frac{1}{\tau_p}[f_i-f_i^{(eq)}], \tag{11}$$

but the EDF is now defined by

$$f_i^{(eq)}=\omega_i\rho\left[1+\frac{\boldsymbol{c}_i\cdot\boldsymbol{u}}{c_s^2}+\frac{\boldsymbol{uu}:(\boldsymbol{c}_i\boldsymbol{c}_i-c_s^2\boldsymbol{I})}{2\gamma c_s^4}\right], \tag{12}$$

with $0<\gamma\leqslant 1$ an adjustable parameter. The definition of the fluid density and velocity are the same as Eq. (3).

Through the Chapman-Enskog procedure we can derive the macroscopic equations from the LBE (11) as

$$\frac{\partial\rho}{\partial t}+\nabla\cdot(\rho\boldsymbol{u})=0, \tag{13a}$$

$$\frac{\partial(\rho\boldsymbol{u})}{\partial t}+\frac{1}{\gamma}\boldsymbol{\nabla}\cdot(\rho\boldsymbol{uu})=-\frac{1}{\gamma}\boldsymbol{\nabla}p^*+\frac{1}{\gamma}\nabla\cdot(\rho\nu\boldsymbol{S}), \tag{13b}$$

where $p^*=\gamma c_s^2\rho$, and $\nu=\gamma c_s^2(\tau_p-0.5)\delta_t$. Clearly, for steady flows, Eq. (13) reduces to Eq. (5), but with a different equation of state. It is clear that the effective sound speed $c_s^*=\sqrt{\partial p^*/\partial\rho}=\sqrt{\gamma}c_s$ is decreased as $\gamma<1$.

It should be noted that if there exists a body force $\boldsymbol{F}$ acting on the fluid, the PLBE (11) should be modified by adding a forcing term $\delta_t F_i$ on its the right-hand side. Several choices for the forcing term are available in literature for the standard LBE (see, e.g., [27] and references therein), and similar formula for F_i can also be applied to the present PLBE, but with a scaled body force by γ. For instance, if we ignore the higher order terms in F_i, we can express it as $F_i=\omega_i\boldsymbol{c}_i\cdot\boldsymbol{F}/\gamma c_s^2$. With such a forcing term, the resultant momentum equation takes the same form as Eq. (13b) except with a scaled body force $\boldsymbol{F}/\gamma$.

The macroscopic equations (13) can be interpreted as preconditioned Navier-Stokes equations. In fact, Eq. (13) can be rewritten as

$$\frac{\partial\boldsymbol{Q}}{\partial t}+\boldsymbol{PA}\frac{\partial\boldsymbol{Q}}{\partial x}+\boldsymbol{PB}\frac{\partial\boldsymbol{Q}}{\partial y}=\boldsymbol{PR}\{\boldsymbol{Q}_v\}, \tag{14}$$

where $\boldsymbol{Q}$, $\boldsymbol{A}$, $\boldsymbol{B}$, and $\boldsymbol{R}$ are the same as defined earlier, except that c_s is replaced by the effective sound speed c_s^*; $\boldsymbol{P}=\mathrm{diag}(1,1/\gamma,1/\gamma)$ is a precondition matrix. Now the eigenvalues of the preconditioned convection matrix $\boldsymbol{PA}$ become

$$\lambda(\boldsymbol{PA})=(u,u\pm\overline{c_s})/\gamma, \tag{15}$$

where $\overline{c_s}=u\sqrt{1-\gamma+(\gamma c_s/u)^2}$ is an effective sound speed. It is clear that as $\gamma=1.0$, $\overline{c_s}$ reduces to the original sound speed c_s. Conversely, as γ approaches zero, $\overline{c_s}$ approaches the fluid speed u. Therefore, by adjusting this parameter, we can decrease the disparity between the speeds of the acoustic wave and the waves propagating with the fluid velocity, and thus accelerate the convergence rate of the LBE. It is also noted that for low Mach number flows, namely, as $u\to 0$, we have $\overline{c_s}=c_s^*=\sqrt{\gamma}c_s$.

According to the effective sound speed c_s^*, we can define an effective Mach number M^* as $M^*=U_0/c_s^*$. It is clear that $M^*=\sqrt{\gamma}M$, and, therefore, $M^*\geqslant M$ for $0<\gamma\leqslant 1$. In practical applications, the parameter γ can be chosen such that M^* is low enough for a given flow condition. This can be done by first specifying the value of M^* according to the flow condition and then setting $\gamma=(M/M^*)^2$.

B. Linear stability analysis

The parameter γ has an influence on the stability of the PLBE. In fact, from the relationship between the viscosity and the relaxation time, we obtain

$$\tau_p-0.5=\frac{\sqrt{3}NM}{\gamma\mathrm{Re}}, \tag{16}$$

from which we see that the deviation of τ_p from 0.5 is increased by decreasing the value of γ for given M and Re on a fixed lattice. Therefore, it is expected that the PLBE (11) has a better numerical stability range than the standard LBE (1) for small Mach number or high Reynolds number flows. It is also noted that γ also influences $f_i^{(eq)}$. The decrease in γ means an increase in the last term in the brackets of the EDF given by Eq. (12), which may make EDFs become negative and, thus, cause numerical instability. These arguments indicate that the parameter γ has complicated influences on the numerical stability of the PLBE.

The stability of the PLBE can be analyzed systemically using the von Neumann linear analysis method [26]. To this end, we first expand the DF $f_i(\boldsymbol{x},t)$ as

$$f_i(\boldsymbol{x},t)=\overline{f_i^{(0)}}+f_i'(\boldsymbol{x},t), \tag{17}$$

where the global EDF $\overline{f_i^{(0)}}$ is a constant that depends only on the constant uniform density ρ_0 and velocity $\boldsymbol{u}_0$, $f_i'(\boldsymbol{x},t)$ is the fluctuation of f_i around the global EDF. Substituting this expansion into the LBE (11), we obtain a linearized system,

$$f_i'(\boldsymbol{x}+\boldsymbol{c}_i\delta_t,t+\delta_t)-f_i'(\boldsymbol{x},t)=-\frac{1}{\tau_p}[f_i'(\boldsymbol{x},t)-G_{ij}f_j'(\boldsymbol{x},t)], \tag{18}$$

where $G_{ij}=\partial f_i^{(eq)}(\rho_0,\boldsymbol{u}_0)/\partial f_j$ is the Jacobian matrix evaluated at the uniform mean density and velocity. It is noted that G_{ij} does not vary in space or time. Equation (18) can be rewritten in a compact form as

$$f_i'(\boldsymbol{x}+\boldsymbol{c}_i\delta_t, t+\delta_t) = M_{ij} f_j'(\boldsymbol{x}, t), \tag{19}$$

where the matrix M_{ij} is given by

$$M_{ij} = \left(1 - \frac{1}{\tau_p}\right)\delta_{ij} + \frac{1}{\tau_p} G_{ij}. \tag{20}$$

The Fourier transform of Eq. (19) gives that

$$F_i(\boldsymbol{k}, t+\delta_t) = \exp[-i\boldsymbol{k}\cdot\boldsymbol{e}_i] M_{ij} F_j(\boldsymbol{k}, t), \tag{21}$$

where $i=\sqrt{-1}$, $F_j(\boldsymbol{k},t)$ is the Fourier transform of $f_i'(\boldsymbol{x},t)$, $\boldsymbol{k}$ is the wave number in units of $1/\delta_x$, and $\boldsymbol{e}_i=\boldsymbol{c}_i/c$ is the dimensionless discrete velocity. The spatial dependence of the stability of the PLBE (11) is determined by the eigenvalues of the matrix $\Gamma_{ij}(\boldsymbol{k})=\exp[-i\boldsymbol{k}\cdot\boldsymbol{e}_i]M_{ij}$. The explicit expression of the Jacobian matrix G_{ij} for the D2Q9 model can be written as

$$G_{ij} = \omega_i \Bigg[1 + 3(\boldsymbol{e}_i\cdot\boldsymbol{e}_j) - \frac{3}{2\gamma}(2(\boldsymbol{e}_j\cdot\boldsymbol{u}_0') - u_0'^2) + \frac{9}{2\gamma}(2(\boldsymbol{e}_i\cdot\boldsymbol{u}_0')(\boldsymbol{e}_i\cdot\boldsymbol{e}_j) - (\boldsymbol{e}_i\cdot\boldsymbol{u}_0')^2) \Bigg], \tag{22}$$

where $\boldsymbol{u}_0'=\boldsymbol{u}_0/c$. It can be shown that the eigenvalues of G are 1 and 0 with multiplicities 3 and 6, respectively, which are independent of γ and $\boldsymbol{u}_0'$. Accordingly, the eigenvalues of the matrix M are 1 and $1-1/\tau_p$.

It is clear that $\Gamma=M$ as $\boldsymbol{k}=\boldsymbol{0}$; therefore, the PLBE (11) is asymptotically stable if $|1-1/\tau_p|<1$, i.e., $\tau_p \geqslant 0.5$, which is the same as the standard LBE [26]. As $\boldsymbol{k}\neq 0$, the eigenvalues of Γ has a complex dependence on the parameters γ, $\boldsymbol{u}_0'$, $\boldsymbol{k}$, and τ_p. Hence, it is rather difficult to give a complete mapping of all the stability boundaries. Here we restrict ourselves to cases where the wave number $\boldsymbol{k}$ is parallel to the uniform velocity $\boldsymbol{u}_0$ because under such circumstances the most unstable condition occurs for the standard LBE [26]. Furthermore, we assume that both $\boldsymbol{k}$ and $\boldsymbol{u}_0$ are aligned with $\boldsymbol{e}_1$. It is also noted that for a given lattice and fixed M and Re, the dimensionless relaxation time τ_p should be adjusted according to Eq. (16) for different values of γ. In fact, τ_p can be determined by

$$\tau_p - 0.5 = (\tau_s - 0.5)/\gamma, \tag{23}$$

where τ_s is the relaxation time for the standard LBE as $\gamma=1$.

We first investigate the dependence of the modulus of $\Gamma(k)$, the maximum magnitude of the eigenvalues of $\Gamma(k)$ [denoted as $\|\Gamma(k)\|$], on the wave number k. We note that for small values of u_0', as γ decreases from 1 to a certain critical value larger than zero, $\|\Gamma(k)\|$ becomes smaller at all wave numbers in comparison to the case for $\gamma=1.0$. However, as γ is lower than the critical value, $\|\Gamma(k)\|$ increases dramatically at some wave number and the numerical stability becomes worse. As an example, we present in Fig. 1 the modula of Γ with $\boldsymbol{u}_0'=0.01$ and $\tau_s=0.501$ for several different values of γ.

The global stability of the proposed PLBE model relies on the maximum value of $\|\Gamma(k)\|$ over the entire range of k (referred to as λ_m). In Fig. 2, λ_m is plotted as a function of τ_s and u_0' for several values of γ. It is first observed that for

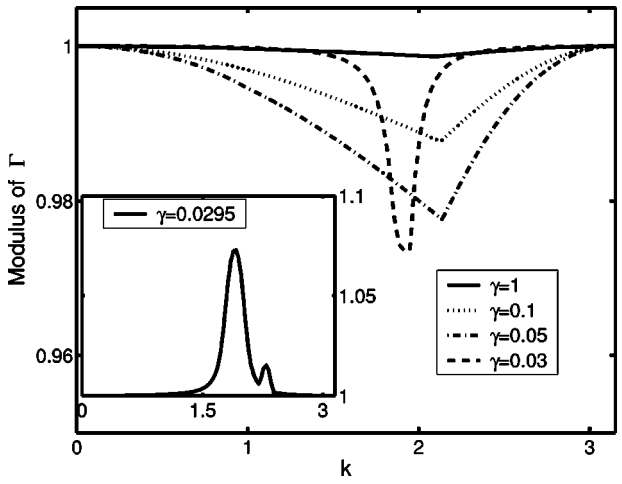

FIG. 1. The modulus of Γ vs wave number k for different γ. $\mathbf{u}_0'=0.01$ and $\tau_s=0.501$.

each value of γ, there exists a critical value u_{0c}'. As $u_0' \leqslant u_{0c}'$, $\lambda_m \leqslant 1.0$, and the PLBE would be stable. On the contrary, as $u_0' > u_{0c}'$, λ_m increases dramatically with u_0' and the scheme would become unstable. This critical value clearly depends on the parameter γ: the smaller γ is, the smaller u_{0c}' is, which means that the stable range of PLBE is reduced as compared to the case for $\gamma=1$ (i.e., the standard LBE). Fortunately, for small Mach number flows in which LBE works, the fluid velocity is usually much lower than $\boldsymbol{u}_{0c}$, and under such a circumstance the PLBE is expected to have a stability similar to the standard LBE.

IV. NUMERICAL EXAMPLES

In this section, some numerical simulations are carried out to demonstrate the performance of the proposed PLBE. In all runs, we assume that the steady state is reached as the residual error $\epsilon(t) \equiv \|u(t)-u(t-100\delta_t)\|_2 / \|u(t)\|_2$ is less than 10^{-6}, where $u(t)$ is the computed velocity field at time t.

A. Couette flow

We first apply the PLBE to the planar Couette flow in a channel where the upper plate moves with a constant veloc-

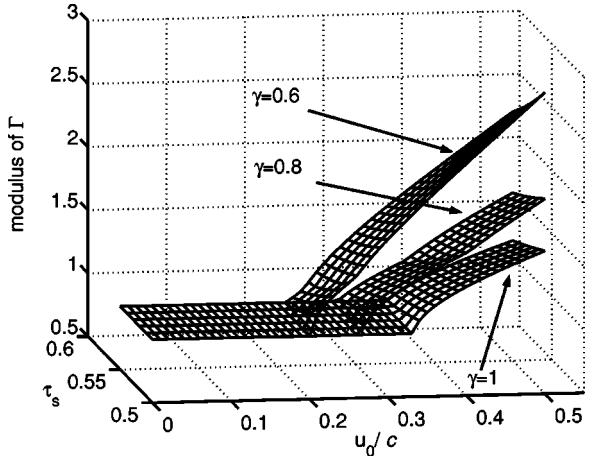

FIG. 2. The maximum modulus of Γ vs τ_s and $\mathbf{u}_0/c$ for different γ.

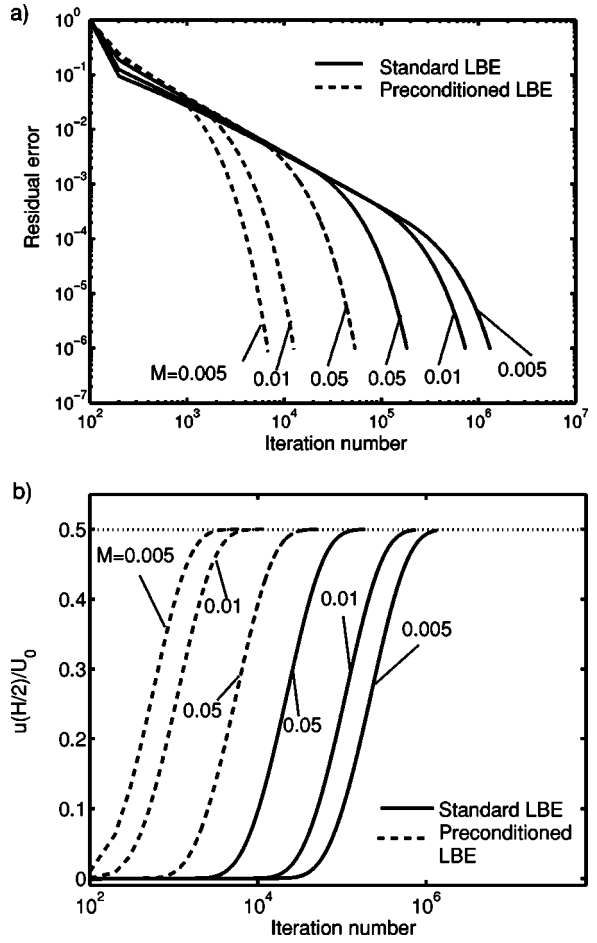

FIG. 3. Convergence histories of PLBE and standard LBE for the Couette flow with different Mach numbers. Re=100, $M^*=0.1$: (a) residual error, (b) velocity at the channel center.

ity U_0 relative to the bottom plate. An analytical solution is known for this problem and, thus, enables us to compare the accuracy of the PLBE with the standard LBE. In simulations, a periodic boundary condition is applied to the entrance and exit, and the nonequilibrium extrapolation method for velocity boundary condition [28] is applied to the top and bottom plates. All the simulations are carried out on a 64×64 lattice. Initially, the velocity in the entire channel is set to zero, and the density is set to unity. The Reynolds number based on U_0 and the channel width H is fixed at 100.0, and the precondition parameter γ is set to be $\gamma=(M/M^*)^2$ with different values of M and M^*.

The convergence processes for various M of the PLBE with $M^*=0.1$ are presented in Fig. 3 together with the results of the standard LBE. In simulations, the channel width H is fixed and the relaxation time τ_p is adjusted to keep the same Reynold number Re. It is seen that in all cases the PLBE converges to the exact solution with a faster rate than the standard LBE, and the acceleration depends on γ. As expected, the smaller M, the more slowly the standard LBE converges. On the contrary, the smaller the M, the faster the preconditioned LBE converges. This feature is further demonstrated in Fig. 4 with some other values of M^*, which indicates that the relation between the iteration number

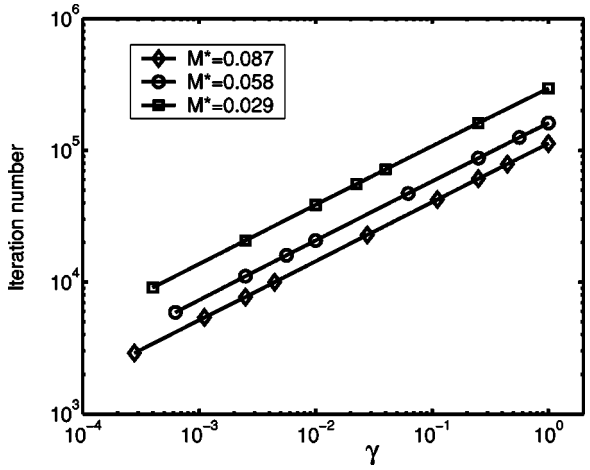

FIG. 4. The iteration number vs γ for the Couette flow at various reference Mach numbers. Re=100.

needed to reach the steady state can be expressed approximately as $N\sim\gamma^n$ with $n\approx0.45$, for the case under consideration. Figure 4 also shows that the convergence rate of the PLBE with $M<M^*$ and $\gamma=(M/M^*)^2$ is enhanced to that of the standard LBE with $M=M^*$ and $\gamma=1.0$, although in both cases the effective Mach number is identical.

Another gain of the PLBE is the improvement in accuracy. The global relative error, defined by $E=\|u-u_e\|_2/\|u_e\|_2$ with u as the numerical solution and u_e as the analytical solution, is displayed in Fig. 5 against γ with different reference Mach numbers. As seen, the errors decrease exponentially with γ in all cases considered, which demonstrates the accuracy improvement of the PLBE, although in all cases the effective Mach number is identical.

The above findings are of practical significance: to obtain the solution of a Steady flow problem economically and accurately, should we use the standard LBE with a relatively larger Mach number or use the PLBE with a smaller Mach number and a larger reference Mach number? The above findings indicate that the PLBE with a smaller Mach number and a smaller γ is a better choice.

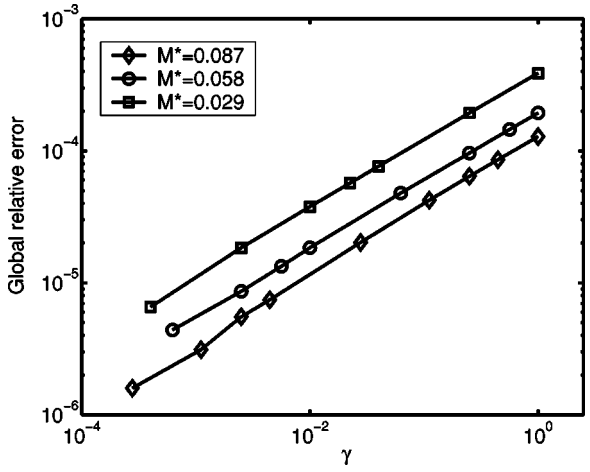

FIG. 5. The global relative error vs γ for the Couette flow at various reference Mach numbers. Re=100.

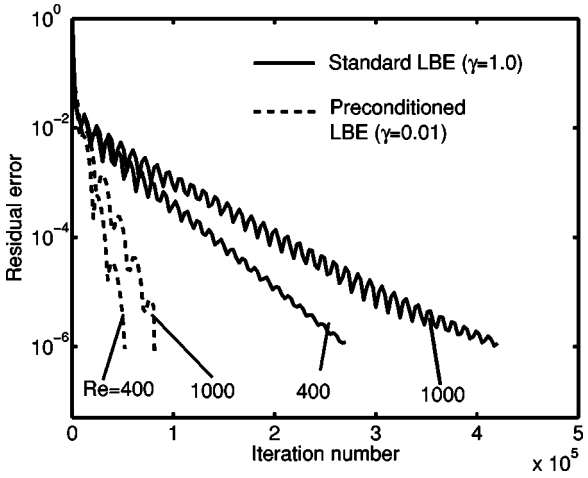

FIG. 6. Convergence histories of PLBE and standard LBE for the cavity flow with Re=400 and 1000. $M^*=0.058$.

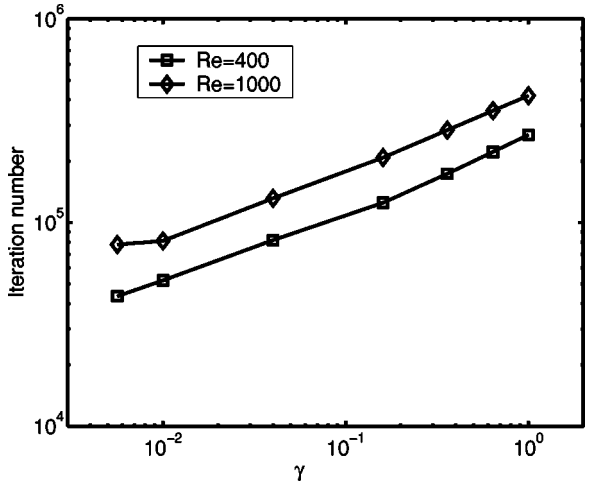

FIG. 7. The iteration number vs γ for the Cavity flow with Re =400 and 1000.

B. Driven cavity flow

The flow in a square cavity whose top wall moves with a uniform velocity U_0 is used as the second test problem for the proposed PLBE. The computational mesh used is 256 $\times$256, and, initially, the fluid is set to be stationary in the whole domain. The nonequilibrium extrapolation method is applied to the four walls to treat the velocity boundary conditions. The reference Mach number M^* is set to be 0.058, and the precondition parameter γ is changed according to the Mach number M as before.

Computations were carried out for Re=400 and 1000, where Re is the Reynolds number based on U_0 and the cavity height H. In Fig. 6, the time-history of the residual errors for each case is presented, and the result for the standard LBE is

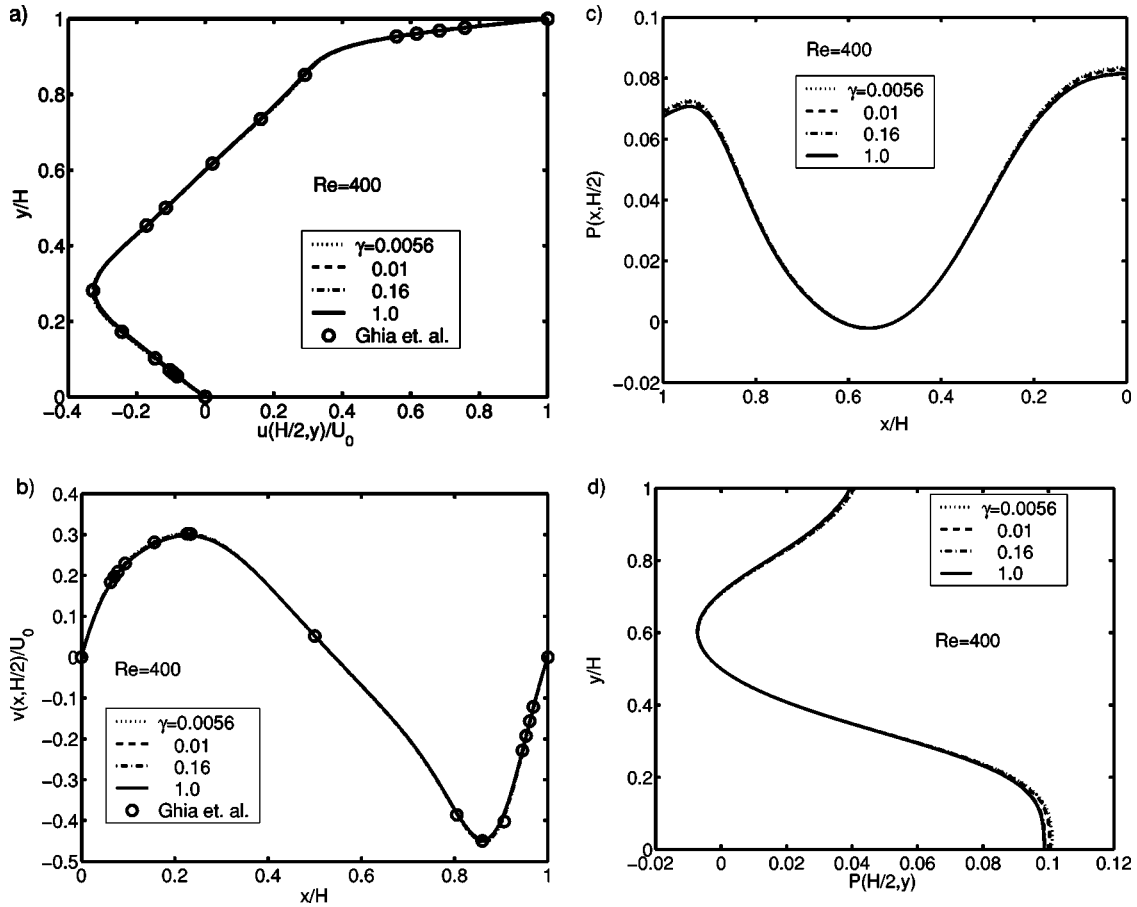

FIG. 8. Velocity [(a) and (b)] and pressure [(c) and (d)] distributions through the cavity center at Re=400.

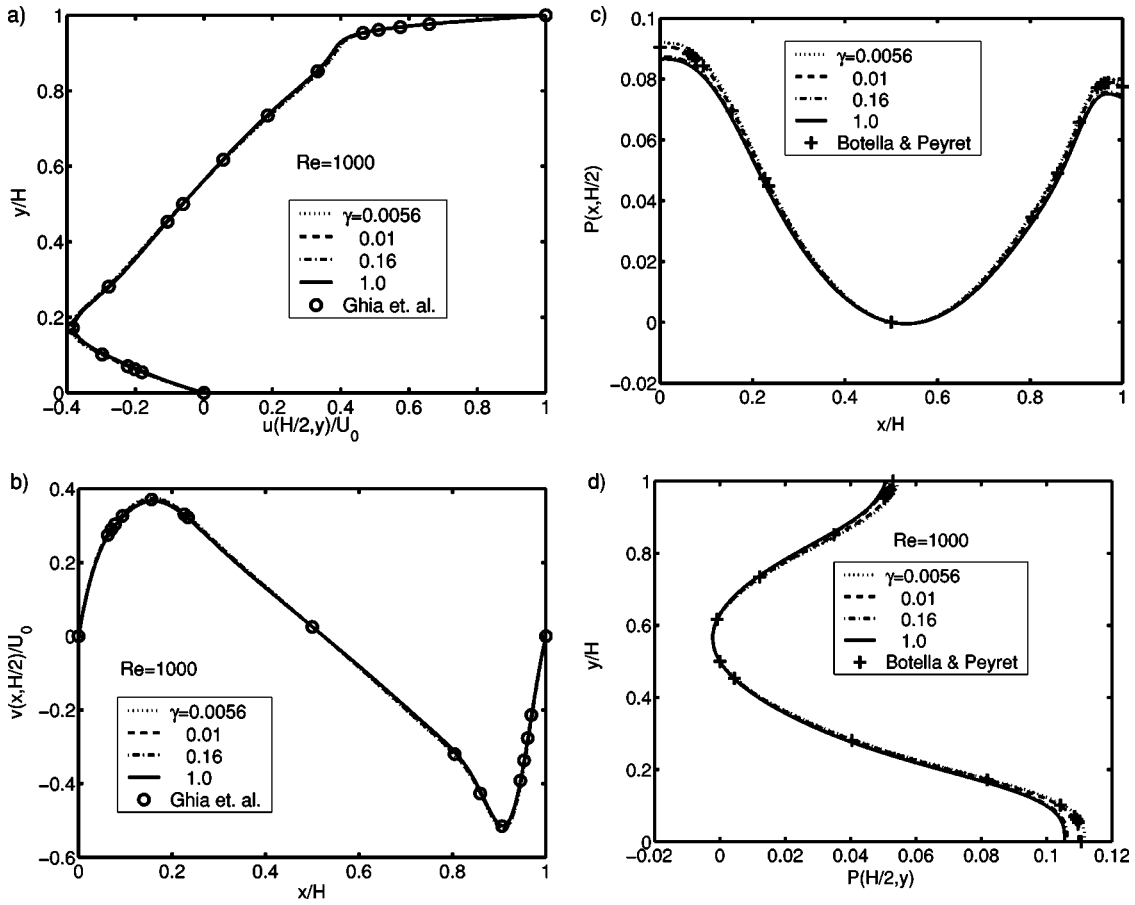

FIG. 9. Velocity [(a) and (b)] and pressure [(c) and (d)] distributions through the cavity center at Re=1000

also presented for comparison. It is clearly seen that the PLBE enhanced the convergence rate greatly for both cases compared with the standard LBE. Usually, the convergence acceleration depends on γ for a given Re, as illustrated in Fig. 7.

It should be emphasized that the acceleration of PLBE is achieved without sacrificing the accuracy of the solution. In Figs. 8 and 9, the velocity and pressure distributions along the vertical and horizontal lines through the cavity center are presented for Re=400 and 1000, together with the benchmark results if available [29,30]. It is seen that in all cases the velocity distributions predicted by the PLBE agree well with the benchmark solutions, and the difference between these results with different γ is nearly indistinguishable. However, some prominent differences are observed among the pressure distributions for different values of γ. The differences are small in the central region, but become larger near the walls. Also, the differences increase as Re becomes larger. The comparison with the benchmark data [30] shows that the pressure distributions predicted by the PLBE with $\gamma<1$ agree better with the benchmark solutions than that by the standard LBE ($\gamma=1$), which demonstrates the desirable properties of PLBE.

It is noted that some oscillations occurs during the convergence process. This is due to the reflection of the acoustic waves on the walls. We find that this oscillation can be damped out by enhancing the bulk viscosity, which does not alter the solutions for incompressible flow or compressible flow with low Mach number. The suppression of such oscillations can further accelerate the convergence process. We will address this problem elsewhere.

V. SUMMARY

The standard LBE method is usually ineffective for steady flows due to the slow convergence rate. In this paper, a preconditioned LBE with an accelerated convergence rate is proposed. For steady flows, the macroscopic equations derived from the model are equivalent to the Navier-Stokes equations, but with an improved eigenvalue system. Numerical tests have been carried out to verify the convergence behavior and numerical accuracy of the model. The results indicate that the preconditioning can improve the convergence rate greatly, while maintaining or even improving the accuracy of the final results predicted by the standard LBE. The convergence rate can be accelerated by orders of magnitude, depending on the parameter γ.

The main difference between the present LBE model and other accelerated time-marching LBE methods [11–15] lies in the definitions of the EDFs. In all of the previous models, the EDF is the same as that used in the standard LBE, and the acceleration is achieved by employing heuristic technique [11,12] or complicated implicit schemes [13–15]. The eigenvalue stiffness of the derived macroscopic equations is

unchanged, and the stability and accuracy of these methods need further investigation. The present LBE, however, uses an EDF that differs slightly from the standard one, and all the advantages of the standard LBE are maintained. The acceleration of the PLBE is achieved by decreasing the disparity between the speeds of different waves in the flow, which has a clear physical significance. Furthermore, we can incorporate other acceleration techniques, such as used in Refs. [11–15], into the present PLBE to obtain more efficient methods.

The convergence acceleration of the present PLBE is lower than that of the multigrid LBE proposed in [20]. However, the latter is based on a steady DVBE with the EDF used in the standard LBE. This LBE can be viewed as a multigrid solver for the steady compressible Navier-Stokes equations with low Mach numbers. The equations have an eigenvalue system similar to that of the compressible Navier-Stokes equations derived from the standard LBE, and the eigenvalue stiffness problem still exists. As pointed out in Ref. [8], this eigenvalue stiffness may slow down the convergence rate of a multigrid procedure. A steady DVBE with the EDF defined by Eq. (12), however, can lead to a steady preconditioned Navier-Stokes system, in which the eigenvalue stiffness is softer. Therefore, if we apply the multigrid technique to such DVBE, the resultant multigrid LBE is expected to have better acceleration than that proposed in [20].

In summary, the proposed preconditioned LBE has the following distinctive advantages compared with previous acceleration LBE methods: First, the PLBE converges faster than the standard LBE while maintaining, even improving the accuracy of the solution. Second, the PLBE has the same structure as the standard LBE, except for the slight difference in the EDF, and, hence, the PLBE shares the same advantages as the standard LBE. Finally, the PLBE can serve as a basis to develop more efficient methods by employing other acceleration techniques.

ACKNOWLEDGMENT

The work described in this paper was fully supported by a grant from the Research Grants Council of the Hong Kong Special Administrative Region, China (Project No. HKUST6193/01E).

[1] R. Benzi, S. Succi, and M. Vergassola, Phys. Rep. **222**, 145 (1992).
[2] Y. H. Qian, S. Succi, and S. A. Orszag, in *Recent Advances in Lattice Boltzmann Computing*, edited by D. Stauffer, Annual Reviews of Computational Physics Vol. III (World Scientific, Singapore, 1996), pp. 195–242.
[3] S. Chen and G. D. Doolen, Annu. Rev. Fluid Mech. **30**, 329 (1998).
[4] L-S. Luo, in *Proceedings of Applied Computational Fluid Dynamics, Beijing, 2000*, edited by J-H. Wu (unpublished), pp. 52–83.
[5] S. Succi, *The Lattice Boltzmann Equation for Fluid Dynamics and Beyond* (Oxford University Press, Oxford, 2001).
[6] Y. G. Lai, C. L. Lin, and J. C. Huang, Numer. Heat Transfer, Part B **39**, 21 (2001).
[7] Y.-H. Choi and C. L. Merkle, J. Comput. Phys. **105**, 207 (1993).
[8] E. Turkel, Appl. Numer. Math. **12**, 257 (1993).
[9] D. Lee Ph.D. thesis, University of Michigan, 1996.
[10] E. Turkel, Annu. Rev. Fluid Mech. **31**, 385 (1999).
[11] D. Kandhai, A. Koponen, and A. Hoekstra, J. Comput. Phys. **150**, 482 (1999).
[12] D. Kandhai, A. Hoekstra, and P. M. A. Sloot, Future. Gener. Comp. Sy. 18, 89 (2001).
[13] T. Lee and C. L. Lin, J. Comput. Phys. **185**, 445 (2003).
[14] T. Seta T and R. Takahashi, J. Stat. Phys. **107**, 557 (2002).
[15] J. Tölke *et al.*, Int. J. Mod. Phys. C **9**, 1143 (1998).
[16] R. Verberg and A. J. C. Ladd, Phys. Rev. E **60**, 3366 (1999).
[17] M. Bernaschi, S. Succi, and H. Chen, J. Sci. Comput. **16**, 135 (2001).
[18] M. Bernaschi, S. Succi, H. Chen, and R. Zhang, Int. J. Mod. Phys. C **13**, 675 (2002).
[19] M. Bernaschi and S. Succi, Int. J. Mod. Phys. B **17**, 1 (2003).
[20] J. Tölke, M. Krafczyk, and E. Rank, J. Stat. Phys. **107**, 573 (2002).
[21] Y. Qian, D. d'Humiéres, and P. Lallemand, Europhys. Lett. **17**, 479 (1992).
[22] X. He and L.-S. Luo, Phys. Rev. E **55**, R6333 (1997).
[23] X. He and L.-S. Luo, Phys. Rev. E **56**, 6811 (1997).
[24] S. Hou, Q. Zou, and S. Chen, J. Comput. Phys. **118**, 329 (1995).
[25] Q. Zou, S. Hou, S. Chen, and G. D. Doolen, J. Stat. Phys. **81**, 35 (1995).
[26] J. D. Sterling and S. Chen, J. Comput. Phys. **123**, 196 (1996).
[27] Z. Guo, C. Zheng, and B. Shi, Phys. Rev. E **65**, 046308 (2002).
[28] Z. Guo, C. Zheng, and B. Shi, Phys. Fluids **14**, 2007 (2002).
[29] U. Ghia, K. N. Ghia, and C. T. Shin, J. Comput. Phys. **48**, 387 (1982).
[30] O. Botella and R. Peyret, Comput. Fluids **27**, 421 (1998).